Super Resolution Fluorescence Localization Microscopy

MJ Mlodzianoski, MM Valles, and ST Hess, University of Maine, Orono, ME, USA

Glossary

Localization The two- or three-dimensional positional determination of a point source.

PSF The detection system's characteristic diffraction-limited image of a point source.

Resolution The smallest distinguishable distance between two point sources.

Introduction

Fluorescence microscopy is a popular imaging technique both for its relatively noninvasive properties and its ability to simultaneously image multiple species in living cellular specimens. Images are formed by the simultaneous observation of many fluorescing molecules to visualize cellular structures and processes. In conventional far-field fluorescence microscopy, the spatial resolution is diffraction-limited. Thus, the smallest resolvable details are given by the Rayleigh criterion, namely

$$r_0 \geq \frac{0.61\lambda}{NA}$$

where r_0 is the distance between point sources, λ is the wavelength of the photons detected and NA is the numerical aperture of the lens system (Born and Wolf, 1997). In fluorescence light microscopy, typical lateral and axial resolutions are $\sim$200 nm and $\sim$600 nm, respectively. Thus, in diffraction-limited microscopy, the size and spatial organization of cellular structures on length scales smaller than the diffraction limit remain unresolved.

Many important biological processes occur on length scales shorter than the diffraction limit, and the motivation to improve optical resolution in fluorescence microscopy has been strong. Fortunately, one can observe these phenomena through the use of localization-based super resolution techniques: stochastic optical reconstruction microscopy (STORM) (Rust *et al.*, 2006), photoactivatable localization microscopy (PALM) (Betzig *et al.*, 2006), and fluorescence photoactivation localization microscopy (FPALM) (Hess *et al.*, 2006). These and related techniques have recently become quite popular. Eric Betzig, inventor of PALM, Stefan W. Hell, and William E. Moerner, received the 2014 Nobel Prize in chemistry for their contributions to super resolution microscopy in biological imaging (Nobel Media AB, 2014).

Concept

Localization microscopy is made possible by labeling samples with specific fluorescent molecules that can be converted from a dark to bright state and eventually to another dark (bleached) state (**Figure 1**). Within the sample, an activation laser is used to potentiate the fluorescence of small subsets of single molecules. A second, readout laser excites the fluorescence of those molecules so that they are imaged as diffraction-limited point-spread functions (PSFs) (**Figures 1(a)–1(c)**). During imaging, or, more typically after imaging, the molecular images are mathematically analyzed to determine the two- or three-dimensional coordinates of each identified molecule, which is called localization (**Figures 1(e)–1(g)**). One controls the molecular activation and bleaching rates to allow only a small number of molecules to be visible at once, and to cause those molecules to be separated by a distance greater than r_0. Two-dimensional plots of this information constitute the image (**Figure 1**). Localization microscopy can improve the diffraction-limited resolution by about a factor of 10 or more (**Figures 1(d)** and **1(k)**). This enables the elucidation of biological structures on sub-diffraction length scales.

Localization microscopy can image individual fluorophores as well as multiple fluorophores simultaneously (Bossi *et al.*, 2008; Testa *et al.*, 2010; Gunewardene *et al.*, 2011). Molecular orientations (Gould *et al.*, 2008), and localizations in two or three dimensions (Juette *et al.*, 2008; Huang *et al.*, 2008), can also be determined. Multicolor, molecular orientation and three-dimensional imaging require specific modifications to the detection path, involving the use of specialized optics (**Figure 2**) and methods (see Experimental Methods).

Super resolution imaging can be performed in live cells (Hess *et al.*, 2007) and fixed samples. Fixed cell imaging reveals static information about the size and spatial organization of the labeled structures at one instant in time. Live cell imaging reveals dynamics of cellular structures and enables the measurement of single molecule trajectories on millisecond timescales (Gudheti *et al.*, 2013; Manley *et al.*, 2008).

Experimental Methods

For particular functionalities, the microscope can be aligned to match one of the possible layouts in **Figure 2**. The activation laser, which frequently has a 405 nm wavelength, should be adjusted to spatially overlap with the readout laser. The readout wavelength can be one or several different wavelengths, chosen to best excite the fluorescent molecules in the sample. For example, the photoactivatable fluorescent protein Dendra2 is excited well by a 556 nm or 561 nm laser, whereas Alexa647 is optimally excited at 647 nm. Both lasers are

 doi:10.1016/B978-0-12-394447-4.20090-4

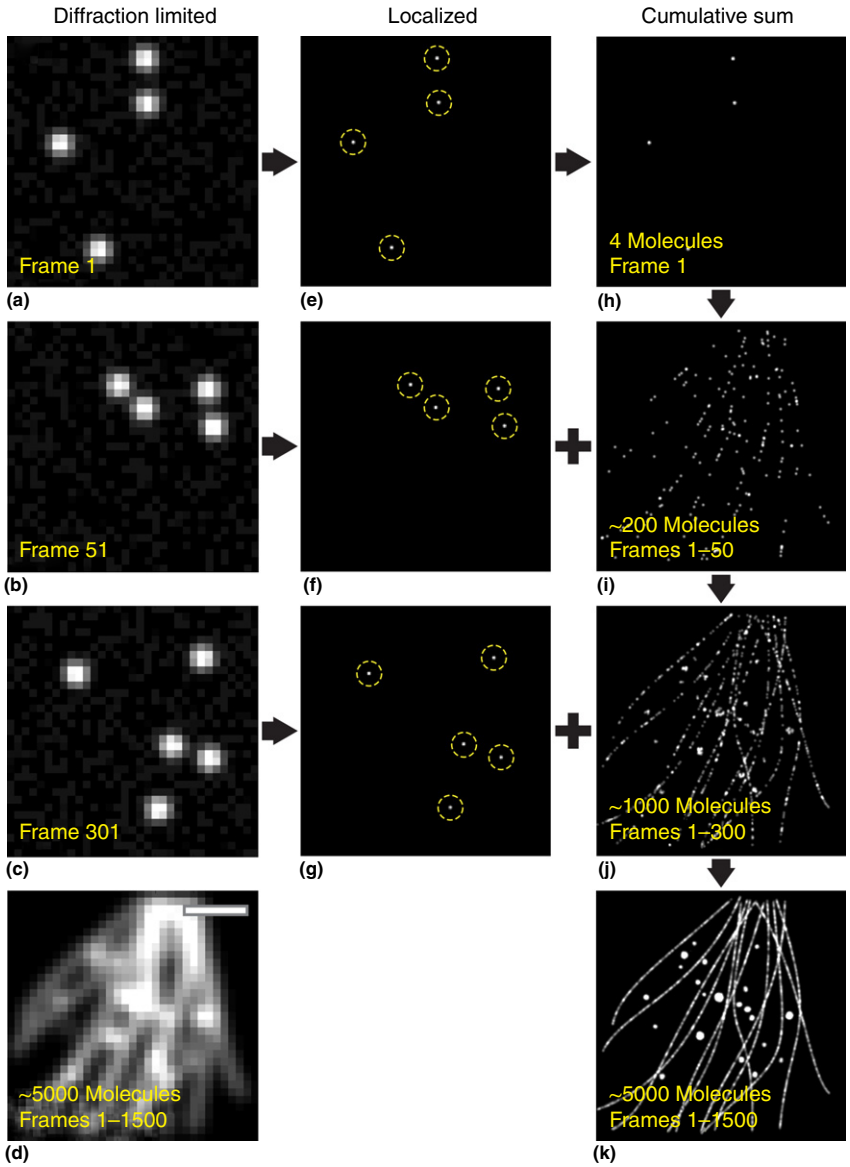

Figure 1 The concept of FPALM is shown using simulated single molecules. Diffraction-limited single molecules are sparsely activated, excited, and imaged before they photobleach (a). Photobleached molecules are replaced in each frame by newly activated single molecules (b,c). Together, all of the single molecules form a diffraction-limited image (d). The recorded single molecules in (a–c) are mathematically localized (e–g, enclosed in yellow circles). The cumulative sum of the localized molecules form super-resolved images (h–k). Sparse numbers of molecules (h,i) do not adequately define the structures as well as larger numbers of molecules (j,k). Scale bar in (d) is 1 μm and is the same for all images.

typically focused by a lens into the back aperture of the objective in order to achieve widefield illumination at the sample.

The lateral position of the laser as it enters the objective affects the excitation profile at the sample. In Figure 2 panel I, the path of the laser lies directly on the optical axis, which results in excitation through the sample. By shifting the path of the laser laterally away from the optical axis, the laser beam becomes inclined in the sample, as seen in panel II. Further shifting of the laser from the optical axis puts the excitation into total internal reflection fluorescence (TIRF) mode, as seen in panel III. In TIRF, the evanescent electric field penetrates only a few hundred nanometers into the sample, enabling excitation of only molecules very close to the surface of the coverslip and greatly reducing out of focus background.

The objective collects a portion of the excited fluorescence, which then passes through the dichroic, and is then focused by the tube lens to form an image in an intermediate plane, where an aperture is placed to crop the area imaged. Two additional lenses form a telescope that magnifies and focuses the cropped image onto the camera. Modifications to the detection path increase the amount of information measured from the single molecules. In Figure 2(a), the fluorescence signal is imaged directly onto the camera and provides two-dimensional spatial information.

Simultaneous multicolor imaging, i.e., the labeling of a sample with multiple spectrally distinct species of fluorescent molecules, can be done using the optical setup shown in Figure 2(b) (Bossi *et al.*, 2008; Testa *et al.*, 2010;

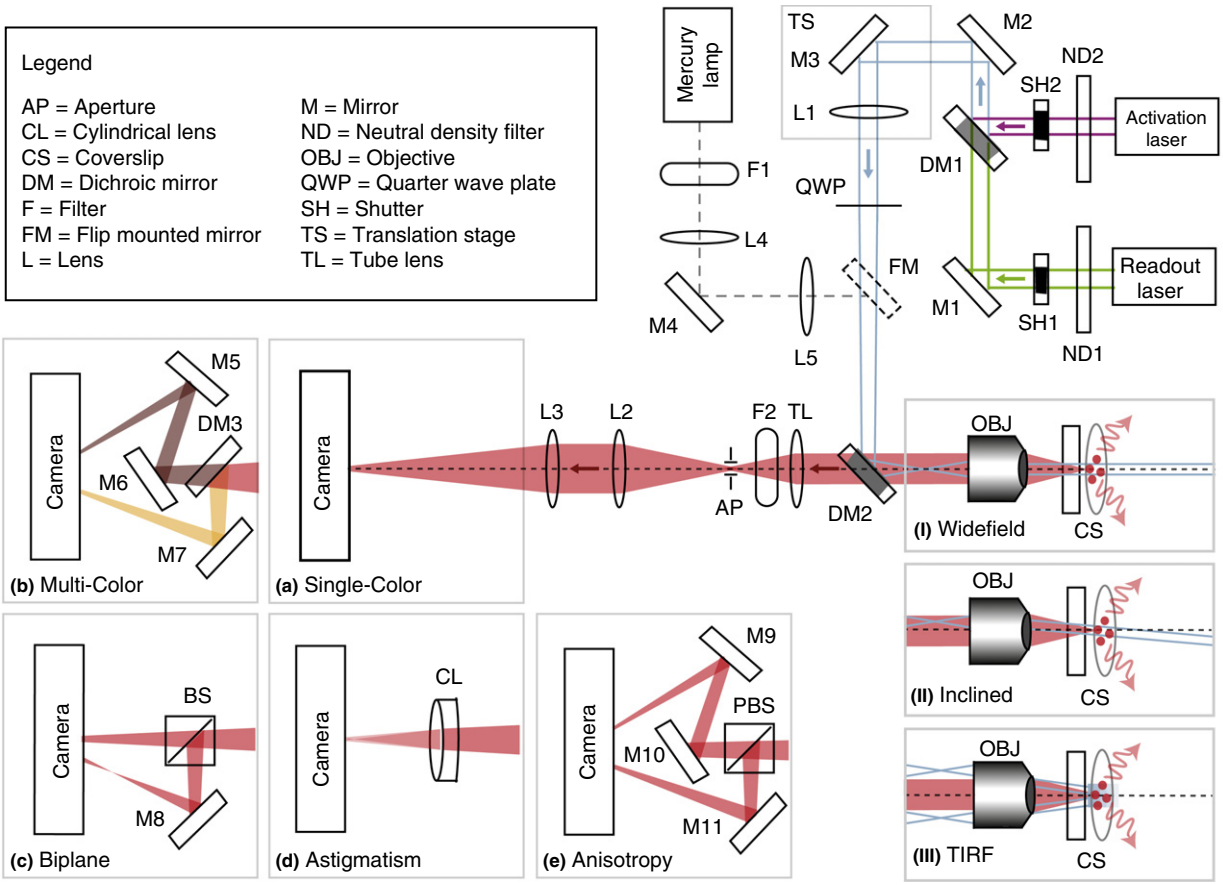

Figure 2 Basic layout of an FPALM setup and many modifications. The Readout and Activation laser on/off and powers are controlled by shutters, SH, and neutral density filters, ND, respectively. The lasers are combined at DM1 and reflected to the lens, L1, by mirrors M2 and M3. The lasers pass through a quarter wave plate, QWP, for conversion to circularly polarized light, then reflect off the filter cube dichroic, DM2, and focus at the back aperture of the objective, OBJ. The lateral position of the lasers at the back aperture of the objective controls the angle at which the lasers enter the sample: (I) centered for excitation perpendicular to the coverslip, (II) slightly offset for inclined beam in the sample, and (III) offset for TIRF. The lateral position of the laser is adjusted by shifting the translation stage, TS. Sample fluorescence is collected by the objective, passes through DM2, and is focused by the tube lens, TL. Outside the microscope, additional bandpass filters, F2, remove background. The aperture, AP, reduces the image region. The image is expanded by the telescope lenses, L2 and L3, before entering the detection box. Modifications to the detection path enable different modes of imaging. For single color imaging, fluorescence is measured directly by the camera (a). For simultaneous multicolor imaging, a dichroic, DM3, separates the fluorescence into two channels (b). Additional mirrors, M5 and M6, ensure the same focal plane is imaged. For three-dimensional imaging by the biplane method, the fluorescence is split by a 50:50 beam splitter, BS, with M8 redirecting reflected fluorescence to the camera (c). The different path lengths result in two different focal planes imaged at the camera. For three-dimensional images by astigmatism, a cylindrical lens is placed in the detection path (d). To measure anisotropy, a polarizing beam splitter, PBS, splits fluorescence depending on polarization, with M9 and M10 ensuring path-length equality (e). Light from the Mercury Lamp passes through a filter, F1, and expands with the telescope lenses L4 and L5. A flip mirror, FM, reflects the mercury lamp light into the microscope.

Gunewardene *et al.*, 2011). The dichroic splits the fluorescence into two color channels and the mirrors adjust the path lengths so that the same focal planes are imaged in side-by-side areas on the camera. The ratio of intensities between the two channels can be used to distinguish the different fluorescent species in the image.

Three-dimensional imaging requires a method to break the axial symmetry of the PSF. Breaking the symmetry can be done by a variety of methods (Juette *et al.*, 2008; Huang *et al.*, 2008; Pavani *et al.*, 2009; Shtengel *et al.*, 2009). Here, we show the two easiest methods to implement: Biplane (Juette *et al.*, 2008) in **Figure 2(c)** and astigmatism (Huang *et al.*, 2008) in **Figure 2(d)**. The Biplane method splits the fluorescence with a 50:50 beam splitter cube so that two different focal planes are imaged on the camera. This provides two separate measurements of the single molecule enabling axial localization. The fluorescence path lengths are different for each channel, resulting in two different focal planes being imaged on the camera. The differences in shape of the molecular images in the two channels enable the localization of the axial position of the molecule. The astigmatism method introduces a cylindrical lens into the detection path as seen in **Figure 2(d)**. The cylindrical lens changes the focal length along only one of the lateral directions. The image of the single molecule will be stretched either horizontally or vertically depending on its axial position. This stretching is then

mathematically modeled to determine the molecular position in three dimensions.

The anisotropy, or dipole orientation, of the imaged single molecules can be measured using the setup in **Figure 2(e)** (Gould *et al.*, 2008). The fluorescence is split by a polarizing beam splitter cube and the mirrors adjust the path lengths so that the same focal planes are imaged on the camera. The ratio of intensities between the two channels enables determination of the azimuthal (in-plane) angle of the dipole of the single molecule.

Preparation of samples can follow standard protocols for fluorescence labeling, however, several crucial details need to be considered. Photoactivatable single molecules, by nature, are sensitive to light. Once labeled, samples should be shielded from stray light sources (room lights, incubator UV, etc) which may prematurely activate single molecules. Additionally, sample media and buffers often contain auto-fluorescent components which serve to increase background noise and worsen the localization precision. Sample media and buffers should be made such that auto-fluorescent components are removed or replaced with nonfluorescent alternatives.

For any multichannel or three-dimensional imaging modality, calibration data should be recorded. Multichannel calibration typically consists of bead images which can be used to create a mathematical transform to overlay the two channels. Three-dimensional calibration data requires precise positioning of beads in order to generate an axial calibration curve.

Data Analysis

Typical localization-based super resolution datasets consist of between a few hundred and several tens of thousands of image frames of single molecules. The crucial point of the technique is to measure spatially well-separated fluorescent single molecules in each frame, as seen in **Figures 1(a)–1(c)**. As the single molecules photobleach and the pool of inactive molecules decreases, the activation intensity should be increased so that the density of active single molecules remains roughly constant during the imaging sequence.

Plots of localized single molecules are shown in **Figures 1(e)–1(g)**. Localization algorithms read in raw data and output a list of localized particle positions. These involve background subtraction before each single molecule is identified and localized. The typical algorithm first involves a calculation of the effective pixel size by using a scale image to determine how many pixels fit in a known image area. Background noise is calculated by measuring the variation of detected fluorescence within a nearby region that does not contain any fluorescing molecules. Single molecules are then identified based on pixel intensity and mathematically localized either by using a least-squares fitting of a Gaussian, maximum-likelihood estimation of a theoretical PSF (Mortensen *et al.*, 2010) or fitting to the experimentally measured PSF (Juette *et al.*, 2008). The identification and localization process repeats for all single molecules in the image. A first set of thresholds are applied to identify objects as bright as a single fluorophore. Objects that pass this first threshold are then localized. A second set of thresholds either discards, or sets aside for further analysis, the PSFs that are substantially larger or smaller than the diffraction limit; or poorly localized based on goodness of fit and number of detected photons. A localization precision is then determined for each PSF to be analyzed, which depends on the number and emission wavelength of the number of photons detected from the fluorophore, the background noise per pixel and the effective pixel size.

For the detection setups in **Figures 2(b)–2(e)**, the analysis algorithms must be modified to extract the appropriate and available information. For multichannel techniques (**Figures 2(b), 2(c),** and **2(e)**), the two channels are overlaid using the calibration data. Single molecules are localized using the methods in the previous paragraph to determine the lateral localized positions. The ratio of intensities and/or the comparison of the shapes of the molecular images in the two channels reveals information such as the type, axial position, or dipole orientation of the single molecule. The images in **Figure 2(d)** form a single channel; the axial positions of the single molecules are extracted by measuring the horizontal and vertical widths of the PSF for each molecule within the image.

A final rendered image of all localized single molecules (**Figure 1(k)**) will have enhanced resolution in comparison to the diffraction-limited image (**Figure 1(d)**). Gaussian-based visualization was used to render the super resolution image in **Figure 1**, but several other methods exist, such as scattergrams, quad-tree histograms, and Delaunay triangulation (Baddeley *et al.*, 2010).

For a more thorough discussion of the microscope setup, alignment, imaging, and analysis methods, see Gould *et al.* (2009), Curthoys *et al.* (2013).

Discussion

Localization microscopy can provide resolution at near molecular length scales, with time resolution of 0.1–0.03 s per rendered image (Huang *et al.*, 2013; Gunewardene *et al.*, 2011; Shim *et al.*, 2012). Because localization microscopy images single molecules, a number of different types of information can be obtained.

Live cell images can be obtained with frame rates of ~1 ms, allowing rendered images to be obtained within 0.1 s for fluorescent proteins (unpublished data) and 0.03 s for organic dyes (Huang *et al.*, 2013). Careful choice of excitation intensity can allow individual molecules to be imaged for multiple frames and thereby single molecule trajectories to be obtained (Gudheti *et al.*, 2013; Manley *et al.*, 2008). From these trajectories, the diffusion or transport behavior of molecular species can be obtained for single species (Hess *et al.*, 2007; Manley *et al.*, 2008), or combinations of species (Gudheti *et al.*, 2013). Multiple molecular species can be distinguished by splitting the detected fluorescence based on wavelength to form two or more simultaneous images, and using the ratio of intensities within those images to determine molecular type (Bossi *et al.*, 2008; Gunewardene *et al.*, 2011; Testa *et al.*, 2010). Alternatively, probes may also be distinguished based on activation or readout wavelength in addition to emission spectrum (Bates *et al.*, 2007). Finally, methods to quantify numbers of molecules or molecular

density are being developed (Manley *et al.*, 2008; Lee *et al.*, 2012; Wolter *et al.*, 2012; Avilov *et al.*, 2014).

Although a wide variety of information can be obtained from a biological sample, a number of parameters must be considered in order to optimize use of localization microscopy for such applications.

The molecular labeling density (**Figures 1(h)–(k)**) and localization have a profound effect on the ultimate quality (and resolution) of images obtained. The localization precision is strongly affected by number of detected photons per molecule, background noise per pixel, camera pixel size, and the width of the diffraction-limited PSF (Thompson *et al.*, 2002). Thus, minimization of fluorescence background and maximization of fluorescence detection efficiency are crucial. Minimization of other sources of image noise, such as pixel-to-pixel (spatial) (Pertsinidis *et al.*, 2010) and frame-to-frame (temporal) variation in camera sensitivity, are also important (Huang *et al.*, 2013). Based on the Nyquist sampling theorem, the density of labels should yield a nearest neighbor distance no larger than half the value of the desired resolution (Shroff *et al.*, 2007). More generally, the resolution can be defined in a number of ways (Betzig *et al.*, 2006; Hess *et al.*, 2006; Mukamel and Schnitzer, 2012; Nieuwenhuizen *et al.*, 2013). Recently, a resolution measure based on information content as a function of spatial frequency has led to a 'Fourier ring correlation' method, which quantifies the effects of localization precision and molecular density for a wide variety of conditions applicable to localization microscopy (Nieuwenhuizen *et al.*, 2013). Use of this method can be made through an ImageJ app.

To optimize image quality, molecular coordinates in localization microscopy datasets need to be corrected for axial and lateral sample drift, such as through the use of fiducials (Betzig *et al.*, 2006), cross-correlation of data subsets (obtained in fixed samples only) (Mlodzianoski *et al.*, 2011), or experimental modifications need to be made to prevent drift during acquisition, such as through autofocus and/or lateral stabilization of the microscope stage relative to the objective lens (Huang *et al.*, 2008).

For multicolor datasets, bleedthrough, defined as inadvertent identification of molecules of one species as another, can cause significant errors in interpretation of results (Kim *et al.*, 2013). Correction for misidentification rates of as little as a few percent is crucial if results are to be used for quantification of colocalization (Kim *et al.*, 2013).

In summary, localization microscopy is well-suited for imaging living and fixed cell specimens, and other biological samples, where fluorescent labels can be attached to the biomolecules of interest, where spatial resolution of tens of nanometers is desirable, and where a time resolution of 0.03 s or slower is sufficient. Molecular trajectories can also be obtained on millisecond timescales. Localization microscopy is to some extent limited by data analysis and the fluorescent labels used for imaging. Without considerable effort, immediate visualization is hindered by the data analysis required. Further development of the fluorescent labels used could further improve temporal and spatial resolution. However, the range of potential biological applications of the technology in its current state is extensive, and further insights into cell biology are likely to result.

Acknowledgments

This work was funded by NIH R15 GM094713, NIH R15 ES024593, NIH R01 AR054170, Maine Technology Institute MTAF 1106 and 2061, the UMaine Office of the Vice President for Research, and the Maine Economic Improvement Fund.

See also: Imaging the Cell: Light Microscopy: Super-Resolution Light Microscopy: Stimulated Emission Depletion and Ground-State Depletion

References

Avilov, S., Berardozzi, R., Gunewardene, M.S., *et al.*, 2014. In cellulo evaluation of phototransformation quantum yields in fluorescent proteins used as markers for single-molecule localization microscopy. Plos One 9 (6), e98362.

Baddeley, D., Cannell, M.B., Soeller, C., 2010. Visualization of localization microscopy data. Microscopy and Microanalysis 16, 64–72.

Bates, M., Huang, B., Dempsey, G.T., Zhuang, X., 2007. Multicolor super-resolution imaging with photo-switchable fluorescent probes. Science 317, 1749–1753.

Betzig, E., Patterson, G.H., Sougrat, R., *et al.*, 2006. Imaging intracellular fluorescent proteins at nanometer resolution. Science 313, 1642–1645.

Born, M., Wolf, E., 1997. Principles of Optics: Electromagnetic Theory of Propagation, Interference and Diffraction of Light. New York, NY: Cambridge University Press.

Bossi, M., Folling, J., Belov, V.N., *et al.*, 2008. Multicolor far-field fluorescence nanoscopy through isolated detection of distinct molecular species. Nano Letters 8, 2463–2468.

Curthoys, N.M., Mlodzianoski, M.J., Kim, D., Hess, S.T., 2013. Simultaneous multicolor imaging of biological structures with fluorescence photoactivation localization microscopy. Journal of Visualized Experiments 9 (82), e50680.

Gould, T.J., Gunewardene, M.S., Gudheti, M.V., *et al.*, 2008. Nanoscale imaging of molecular positions and anisotropies. Nature Methods 5, 1027–1030.

Gould, T.J., Verkhusha, V.V., Hess, S.T., 2009. Imaging biological structures with fluorescence photoactivation localization microscopy. Nature Protocols 4, 291–308.

Gudheti, M.V., Curthoys, N.M., Gould, T.J., *et al.*, 2013. Actin mediates the nanoscale membrane organization of the clustered membrane protein influenza hemagglutinin. Biophysical Journal 104, 2182–2192.

Gunewardene, M.S., Subach, F.V., Gould, T.J., *et al.*, 2011. Superresolution imaging of multiple fluorescent proteins with highly overlapping emission spectra in living cells. Biophysical Journal 101, 1522–1528.

Hess, S.T., Girirajan, T.P.K., Mason, M.D., 2006. Ultra-high resolution imaging by fluorescence photoactivation localization microscopy. Biophysical Journal 91, 4258–4272.

Hess, S.T., Gould, T.J., Gudheti, M.V., *et al.*, 2007. Dynamic clustered distribution of hemagglutinin resolved at 40 nm in living cell membranes discriminates between raft theories. Proceedings of the National Academy of Sciences of the United States of America 104, 17370–17375.

Huang, B., Wang, W.Q., Bates, M., Zhuang, X.W., 2008. Three-dimensional super-resolution imaging by stochastic optical reconstruction microscopy. Science 319, 810–813.

Huang, F., Hartwich, T.M.P., Rivera-Molina, F.E., *et al.*, 2013. Video-rate nanoscopy using sCMOS camera-specific single-molecule localization algorithms. Nature Methods 10, 653–658.

Juette, M.F., Gould, T.J., Lessard, M.D., *et al.*, 2008. Three-dimensional sub-100 nm resolution fluorescence microscopy of thick samples. Nature Methods 5, 527–529.

Kim, D., Curthoys, N.M., Parent, M., Hess, S.T., 2013. Bleed-through correction for rendering and correlation analysis in multi-colour localization microscopy. Journal of Optics 15, 094011.

Lee, S.H., Shin, J.Y., Lee, A., Bustamante, C., 2012. Counting single photoactivatable fluorescent molecules by photoactivated localization microscopy (PALM). Proceedings of the National Academy of Sciences of the United States of America 109, 17436–17441.

Manley, S., Gillette, J.M., Patterson, G.H., *et al.*, 2008. High-density mapping of single-molecule trajectories with photoactivated localization microscopy. Nature Methods 5, 155–157.

Mlodzianoski, M.J., Schreiner, J.M., Callahan, S.P., *et al.*, 2011. Sample drift correction in 3D fluorescence photoactivation localization microscopy. Optics Express 19, 15009–15019.

Mortensen, K.I., Churchman, L.S., Spudich, J.A., Flyvbjerg, H., 2010. Optimized localization analysis for single-molecule tracking and super-resolution microscopy. Nature Methods 7, 377-U59.

Mukamel, E.A., Schnitzer, M.J., 2012. Unified resolution bounds for conventional and stochastic localization fluorescence microscopy. Physical Review Letters 109 (16), 168102.

Nieuwenhuizen, R.P., Lidke, K.A., Bates, M., *et al.*, 2013. Measuring image resolution in optical nanoscopy. Nature Methods 10, 557–562.

Nobel Media AB, 2014. The Nobel Prize in Chemistry 2014 – Press Release. Available at: http://www.nobelprize.org/nobel_prizes/chemistry/laureates/2014/press.html (accessed 08.11.14).

Pavani, S.R.P., Thompson, M.A., Biteen, J.S., *et al.*, 2009. Three-dimensional, single-molecule fluorescence imaging beyond the diffraction limit by using a double-helix point spread function. Proceedings of the National Academy of Sciences of the United States of America 106, 2995–2999.

Pertsinidis, A., Zhang, Y.X., Chu, S., 2010. Subnanometre single-molecule localization, registration and distance measurements. Nature 466, 647-U11.

Rust, M.J., Bates, M., Zhuang, X.W., 2006. Sub-diffraction-limit imaging by stochastic optical reconstruction microscopy (STORM). Nature Methods 3, 793–795.

Shim, S.H., Xia, C.L., Zhong, G.S., *et al.*, 2012. Super-resolution fluorescence imaging of organelles in live cells with photoswitchable membrane probes. Proceedings of the National Academy of Sciences of the United States of America 109, 13978–13983.

Shroff, H., Galbraith, C.G., Galbraith, J.A., *et al.*, 2007. Dual-color superresolution imaging of genetically expressed probes within individual adhesion complexes. Proceedings of the National Academy of Sciences of the United States of America 104, 20308–20313.

Shtengel, G., Galbraith, J.A., Galbraith, C.G., *et al.*, 2009. Interferometric fluorescent super-resolution microscopy resolves 3D cellular ultrastructure. Proceedings of the National Academy of Sciences of the United States of America 106, 3125–3130.

Testa, I., Wurm, C.A., Medda, R., *et al.*, 2010. Multicolor fluorescence nanoscopy in fixed and living cells by exciting conventional fluorophores with a single wavelength. Biophysical Journal 99, 2686–2694.

Thompson, R.E., Larson, D.R., Webb, W.W., 2002. Precise nanometer localization analysis for individual fluorescent probes. Biophysical Journal 82, 2775–2783.

Wolter, S., Loschberger, A., Holm, T., *et al.*, 2012. rapidSTORM: Accurate, fast open-source software for localization microscopy. Nature Methods 9, 1040–1041.